Modeling Oxygen Diffusion and Consumption in a Skin Graft

BENG 221

Aditya Kumar

Vivek Parthasarathy

Kaushik Sridhar

Wun Kiat Justin Tan

10/25/2013

Table of Contents

Background

Every year, 500,000 patients suffer burn injuries requiring treatment in the United States[11], of which the standard medical practice is the application of a skin graft to the burn site in order to lower the risk of infection and dehydration. Skin grafts are also used in the treatment of diabetic leg ulcers and various other skin defects such as venous ulcers and acute injuries[9].

Currently, skin grafts are made available via three major avenues:

1. Transplants
2. Synthetic skin
3. Tissue-engineered skin

Transplants

Skin transplants have been used for over 150 years in clinical practice[7]. Autografts are transplants from other regions of the patient's body, and are preferred because of a reduced risk of rejection and various other complications. Allografts on the other hand, are transplants from a skin donor, which leads to possible rejection or allergic reactions. However, this is still used in cases where large areas of the patient's skin have been damaged or removal of skin from other portions of the patient is not viable. Figure 1 shows two common sites from which skin is harvested for transplants. Lastly, xenografts are where the skin is taken from an animal, usually pig tissue. It is used in the treatment of large wounds when no donor skin is available[2].

Figure 1: Common skin graft harvesting sites for autograft and allograft transplants
Source: http://www.biomed.brown.edu

Synthetic skin

Another alternative to living skin which has been used for skin grafts is the use of an artificial skin substitute. The most common of these consist of collagen matrices which serve to prevent infection and stop the tissue underneath from drying out. Some contain cytokines and growth factors which encourage re-epithelisation and vascularisation[1] but this effect has not been well studied and there is little clinical data on re-epithelisation rates [6].

Tissue engineered skin

Advances in cell culture and tissue engineering have led to the development of tissue engineered skin grafts. These usually involve harvesting of cells which are then cultured and allowed to multiply and grow on a scaffold in order to form a skin substitute. Various companies have developed methods for doing this, and tissue engineered skin products are currently on the market for the treatment of burns and diabetic ulcers. Like transplants, the cells used can be harvested from the patients themselves, a donor, or from other species of animals[1]. In one product Epicel™, a skin biopsy is done to remove the epidermis which is then trypsinized and cultured *in vitro*. When cells have reached confluence they are harvested and attached to gauze dressing for use in a skin graft[5]. Figure 2 shows an illustration of another such method of producing a tissue engineered skin graft developed by Laboratoire D'Organogenese Experimentale in France.

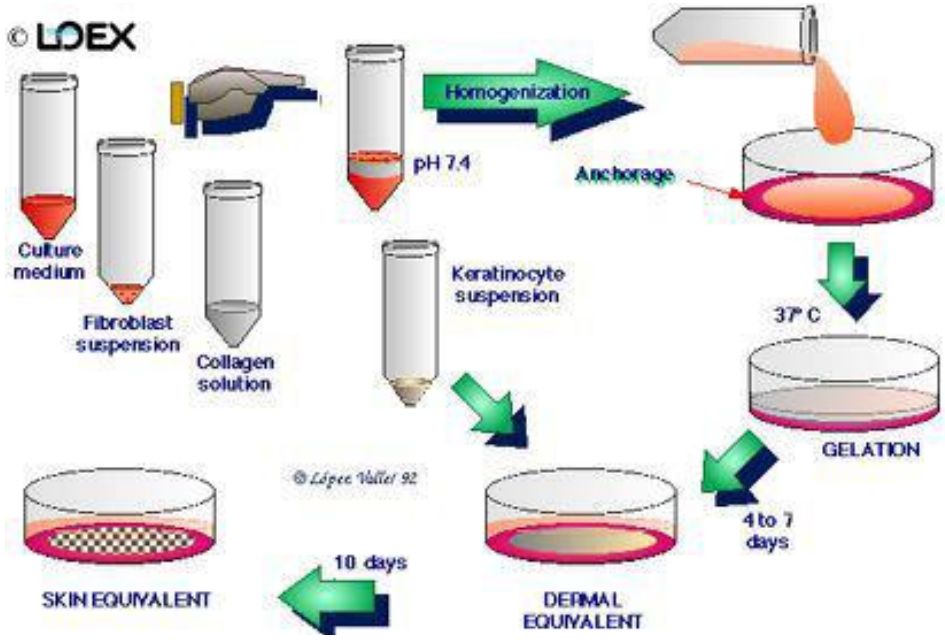

Figure 2. Fibroblasts are suspended in a collagen solution which is allowed to polymerise. Keratinocytes are then seeded on top of the collagen matrix to create a skin equivalent.
Source: http://www.loex.qc.ca/recherche.labos.lrgb.php?langue=2

A major limitation in the culture of engineered tissues and organs is the ability to provide adequate oxygen to the growing cells after they have reached a certain thickness in the absence of vascularisation *in vitro.* Fibroblasts have been shown to require a critical level of oxygen for the secretion and remodelling of collagen, required for the development of a skin graft[8].

Problem statement

The rate of diffusion and consumption of oxygen are major limitations in the culture of cells for use in tissue engineered skin grafts. We aim to model *in vitro* oxygen diffusion and consumption in cultured fibroblasts in an experimental set up similar to that used for the production of tissue engineered skin grafts.

Model and assumptions

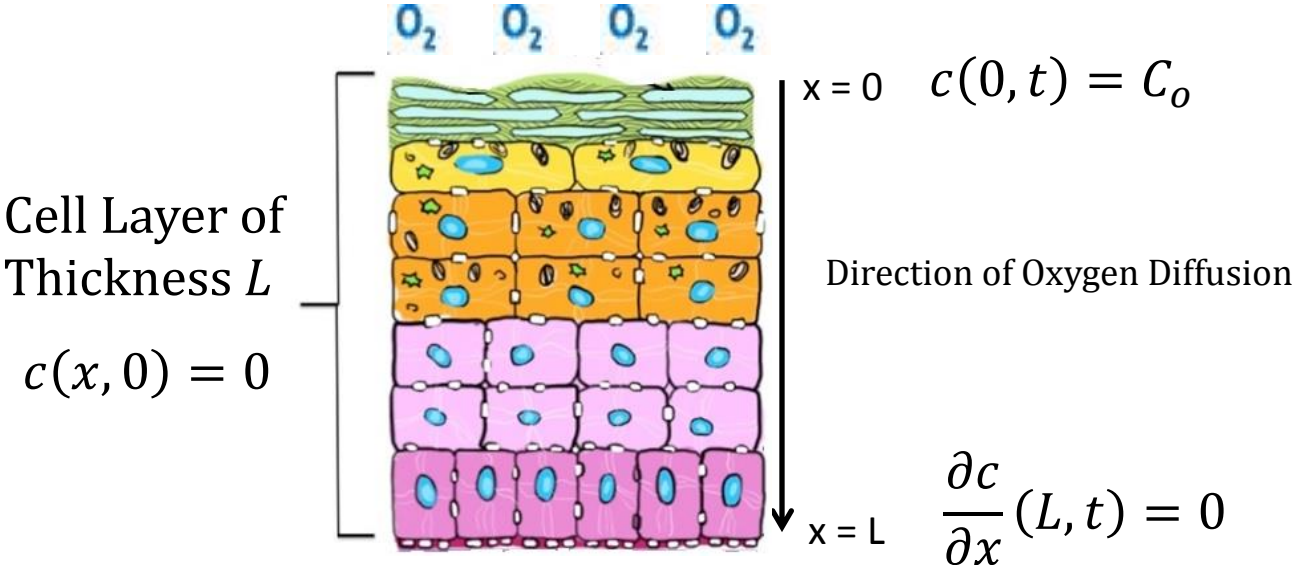

Figure 3. Diagrammatic representation of the model setup. The x-axis points downwards from 0 at the cell surface in contact with air to L at the interface between the cells and the culture vessel. Initial concentration of oxygen throughout is 0mM. Concentration at x=0 is c_0, while flux at x=L is 0.

In order to study the combined effects of diffusion and consumption in tissue cultured cells, we have approximated the system as a homogenous layer of cells growing on the bottom of a tissue culture vessel with thickness L with diffusion in the x direction only. O_2 concentration is constant at the surface of the culture through dissolution of atmospheric oxygen into the media or a constantly moving stream of oxygenated media while flux at the base of the layer if assumed to be 0 due to impermeability of the tissue culture vessel to oxygen. Oxygen is consumed by the cells based on Michaelis-Menten kinetics[3] and travels through the cell layer by diffusion only. For ease of modelling, we have also assumed that no proliferation occurs in the time span of the model and the oxygen consumption is independent of any other factors such as nutrient concentration. Lastly, we have also assumed that the initial concentration of oxygen throughout the cell layer is 0 at time t=0.

The concentration of oxygen in the cell layer can thus be described by the equation

$$\frac{\partial c}{\partial t} = D\frac{\partial^2 c}{\partial^2 x} - \frac{V_m c}{K_m + c} \qquad (1)$$

with initial and boundary conditions

$$I.C.: c(x,0) = 0$$

$$B.C.1: c(0,t) = C_o$$

$$B.C.2: \frac{\partial c}{\partial x}(L,t) = 0$$

where c is the concentration of oxygen, x is the distance from the surface, c_0 is the concentration of oxygen at the surface, D is the diffusivity of oxygen in cells[4], L is the total height of the cell layer, V_m is the maximum rate of oxygen consumption and K_m is the concentration of oxygen at ½ V_m[10]. Values used in our model are given in Table 1.

Table 1. List of parameters used and their values

Parameter	Value
C_0	0.2 [µmol/cm^3]
D	6.6x10^{-6} [cm^2/s]
L	0.02 [cm]
V_m	0.059 [µM/s]
K_m	0.075 [µM]

Homogenous Solution (No consumption)

$$\frac{\partial c}{\partial t} = \frac{\partial^2 c}{\partial x^2} \qquad (2)$$

First, we solved the homogenous equation without consumption in order to get an understanding of the diffusion profile of our system without the consumption term (Appendix A).

Solution: $c(x,t) = C_0 - \sum_{n=0}^{\infty} \frac{4C_0}{(2n+1)\pi} \sin\left(\frac{(2n+1)\pi}{2L} x\right) e^{-\left(\frac{(2n+1)\pi}{2L}\right)^2 Dt}$ (3)

Plotting the analytical solution to the homogenous equation in Matlab (Figure 4), we can see that oxygen diffuses into the cell layer and the oxygen concentration throughout the cell layer eventually reaches steady state c(x) = c0. This is to be expected because of the no flux condition on the other bound.

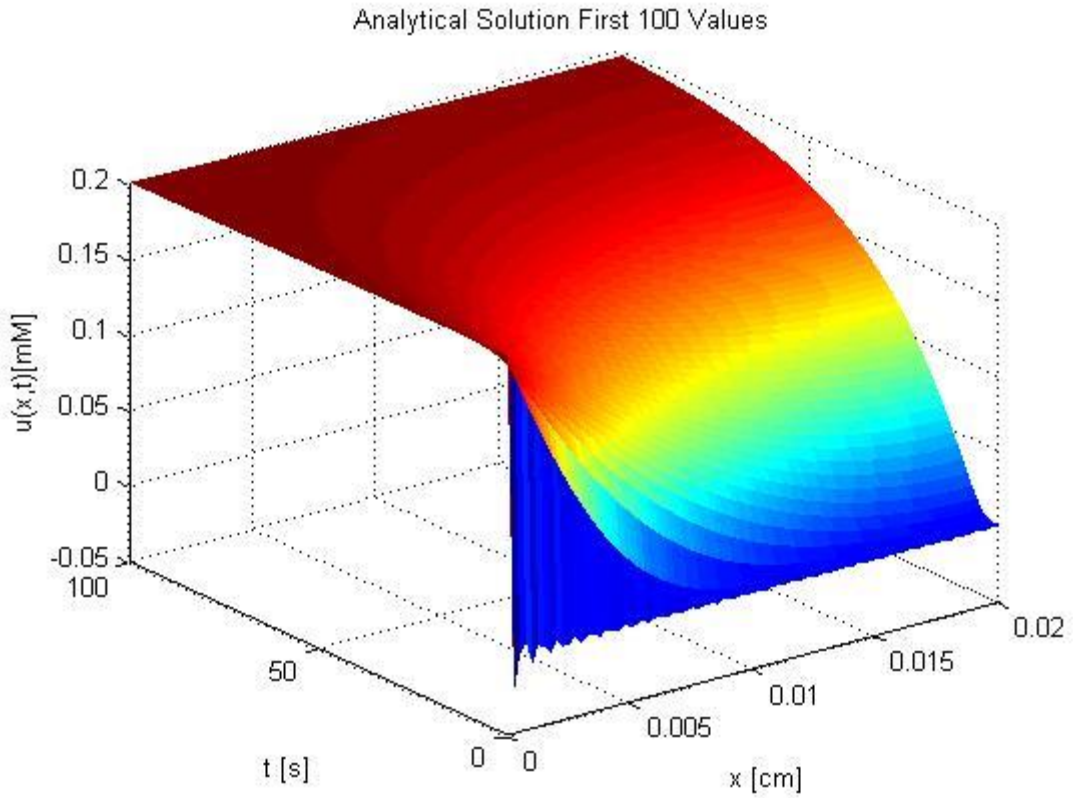

Figure 4. Analytical solution of the homogenous PDE for the first 100 values of n.

Inhomogeneous PDE (Constant Oxygen Consumption)

Analytical Solution

$$\frac{\partial c}{\partial x} = D\frac{\partial^2 c}{dx^2} - R \qquad (4)$$

After solving the homogeneous PDE with inhomogeneous boundary conditions, we incorporated the consumption term into the equation. In order for this equation to be solvable analytically (Appendix B), we modelled oxygen consumption as a constant R, giving us the equation above (Equation 4). As an approximation, this would be true when c>>K_m, hence $\frac{V_m c}{K_m + c} \approx V_m$. Thus, this model incorporates both the oxygen diffusion through the skin graft cell layer in addition to the oxygen consumption term.

Solution:

$$c(x,t) = \frac{R}{2D}x^2 - \frac{RL}{D}x + C_o + \sum_{n=0}^{\infty} B_n \sin\left(\frac{(2n+1)\pi}{2L}x\right)e^{-D\left(\frac{(2n+1)\pi}{2L}\right)^2 t} \qquad (5)$$

The analytical solution was plotted in Matlab and is shown in figures 5 and 6. This solution demonstrated the effects of oxygen concentration throughout the cell layer when factoring in the constant oxygen consumption by the cells.

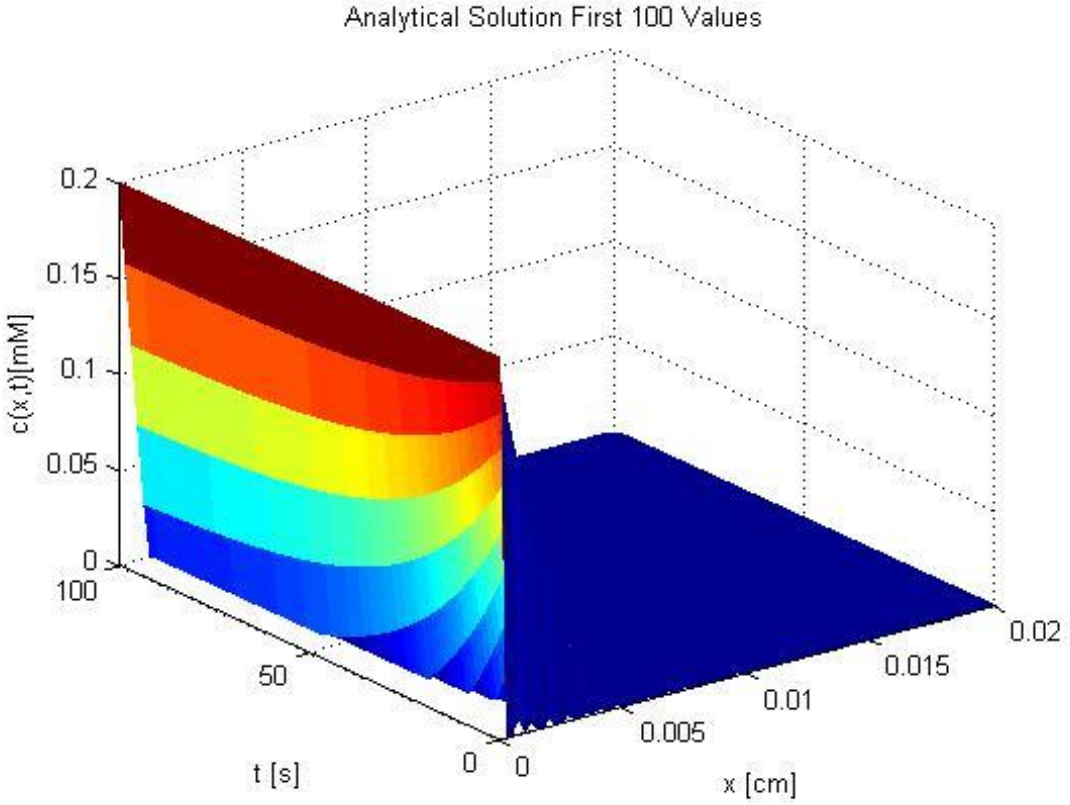

Figure 5. Analytical solution of the inhomogenous PDE with consumption for the first 100 values of n.

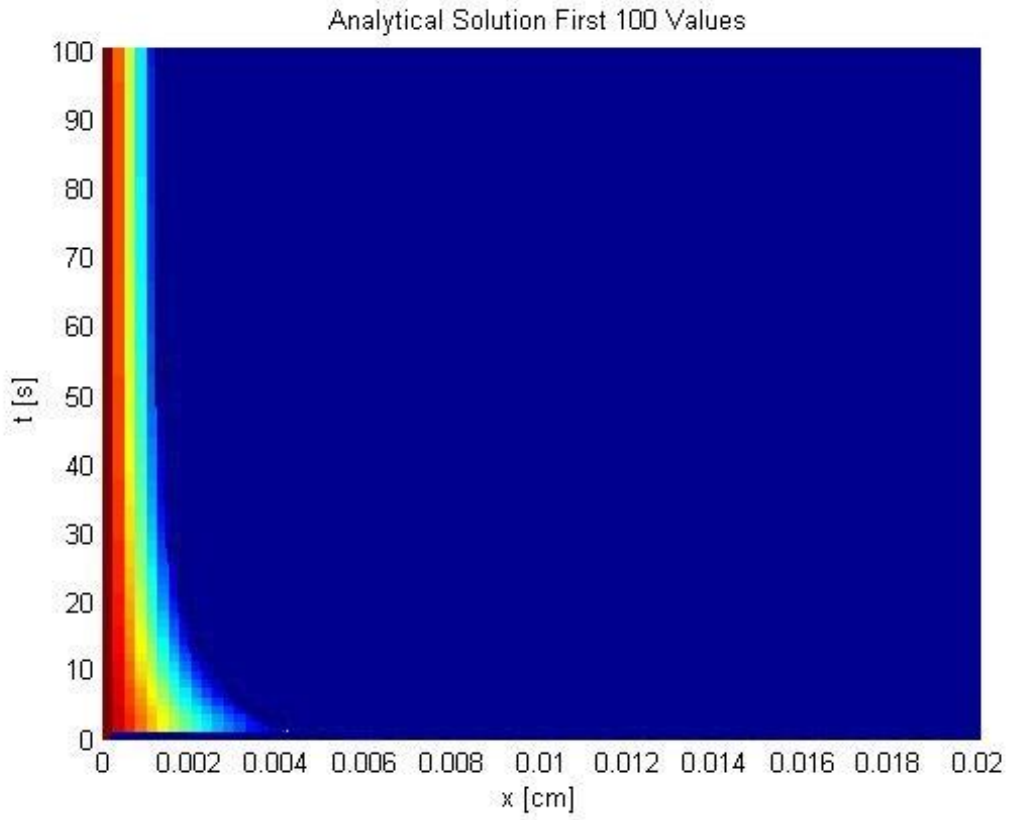

Figure 6. X-Y plane view of the analytical solution to the inhomogenous PDE with consumption for the first 100 values of n.

This plot reveals the dynamics between oxygen diffusion and consumption. As diffusion is proportional to the rate of concentration change, it is initially rapid and oxygen travels about 0.004cm into the cell layer. However, the consumption of oxygen quickly depletes it and the depth of oxygen penetration slowly goes down to 0.002cm at steady state. In Figure 6, the system quickly reaches steady state within fifty seconds and oxygen only appears to diffuse less than 0.002 cm into the cell layer. Additionally, as consumption was not dependent on the concentration, the concentration of oxygen dropped below zero for a large part of the plot. As this is not physically possible, we set the lower limit of oxygen to 0.

Numerical Solution

Next, we used the Finite Differences method in to provide validation of the analytical solution of Equation 4. Surface plots were made using Matlab and are shown in Figures 7 and 8.

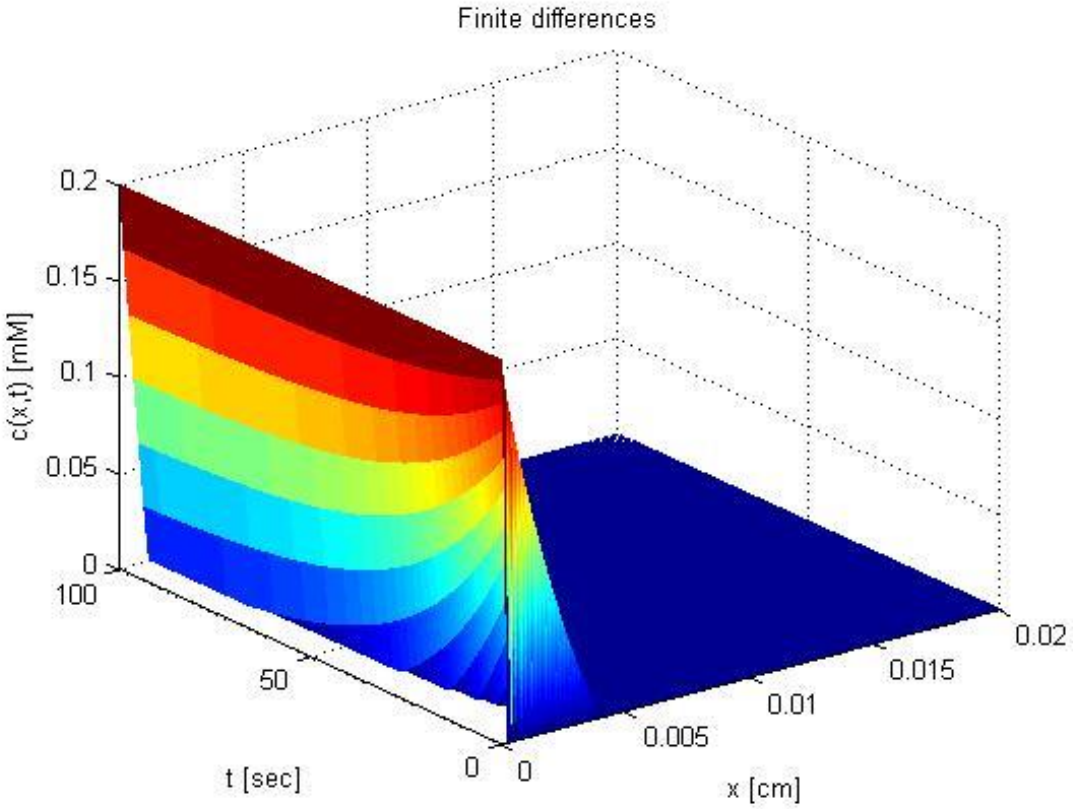

Figure 7. Numerical solution to the inhomogenous PDE with consumption using finite differences method

Figure 7 corroborates well with our analytical solution (Figure 5) which yields a similar result. We observe that the cell layer also quickly reaches steady state within fifty seconds and that oxygen only diffuses about 0.002 cm into the cell layer. Again, we had to set the lower bounds of oxygen concentration in order to make it physically relevant.

An X-Y profile of the above plot (Figure 8) shows that diffusion initially dominates, before consumption brings the system to steady state. It also shows the extent of diffusion of oxygen into the cell layer to be around 0.002 cm, is similar to our analytical solution (Figure 6), showing that in this case the finite difference method is a good approximation of the actual solution (Figure 8).

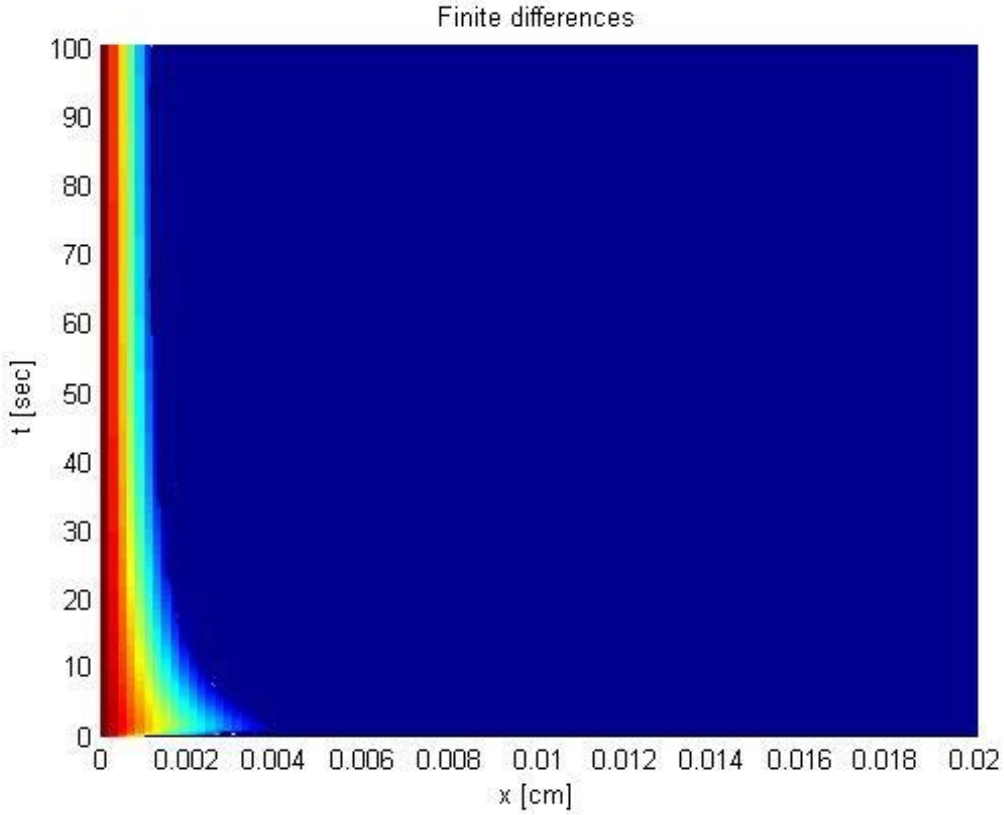

Figure 8. X-Y plane view of the numerical solution to the inhomogenous PDE with consumption using finite differences method

Inhomogeneous PDE (Michaelis-Menten Oxygen Consumption Kinetics)

Given the inaccuracies in the model using the constant oxygen consumption term, we instead modeled oxygen consumption using Michaelis-Menten kinetics to achieve the final equation of our model (Equation 6).

$$\frac{\partial c}{\partial t} = D\frac{\partial^2 c}{\partial x^2} - \frac{V_m c}{K_m + c} \qquad (6)$$

Where V_m is the maximum oxygen consumption rate and K_m is the oxygen concentration at half maximum velocity.

Again, our boundaries and initial conditions are the same as given by equation 1. Using the Finite Differences method, we numerically solved equation 6 and made a surface plot of the solution in Figure 9 and 10.

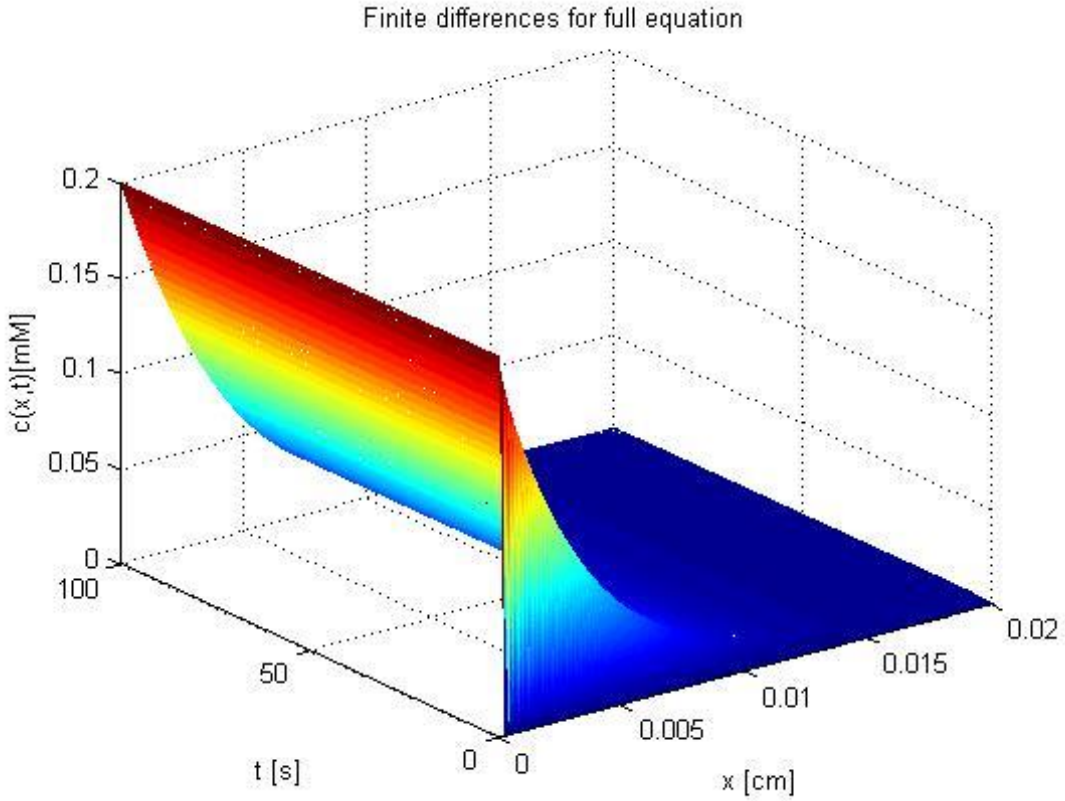

Figure 9. Numerical solution to the inhomogenous PDE with Michaelis Menten consumption using finite differences method

The system reaches steady state much faster using our final equation than when we assumed oxygen consumption was constant. Also, the oxygen diffuses further into the tissue, reaching depths of about 0.018 cm. In this case, because the consumption rate of oxygen is dependent on the concentration, there was no need to set a lower bound on the oxygen concentration. An X-Y profile of the above plot further illustrates the differences between the full equation and the constant consumption equation (Figure 10).

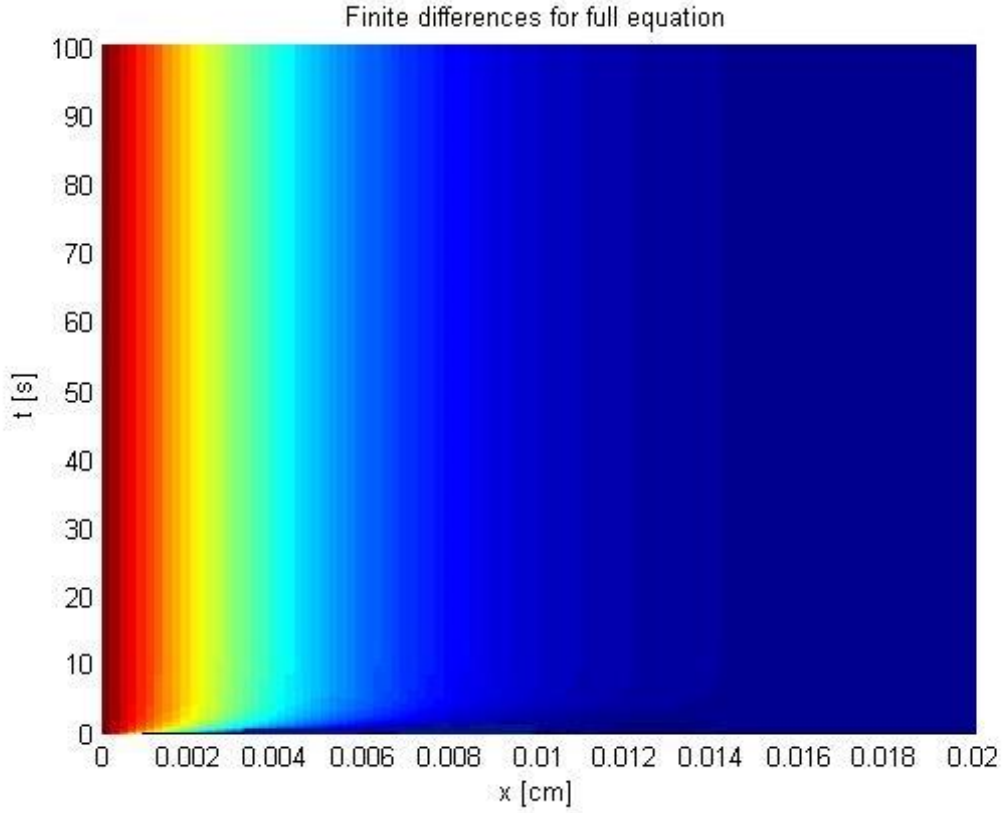

Figure 10. X-Y plane view of the numerical solution to the inhomogenous PDE with Michaelis-Menten consumption using finite differences method

Conclusions

As expected, there was great similarity between the analytical and numerical solutions for the constant oxygen consumption model. In both models, oxygen diffuses about 0.002 cm into the cell layer and reaches steady state within 50 seconds (Figure 6,8). However, the simplification of the oxygen consumption term proved to be inaccurate. This can be demonstrated by looking at the full equation plot in Figure 10. In the full equation, the system reaches steady state much more quickly. In addition, oxygen diffuses about 0.018 cm into the cell layer. Lastly, oxygen concentration never reaches values below zero. This occurred because the consumption term for the full equation is proportional to the oxygen concentration over time. In order to show the stark contrast between the full equation and the simplification, we have plotted the steady states of both equations in Figure 11. As shown, the oxygen concentration for the simplified equation quickly reaches zero whereas the oxygen concentration in the full model ranges throughout the full cell layer.

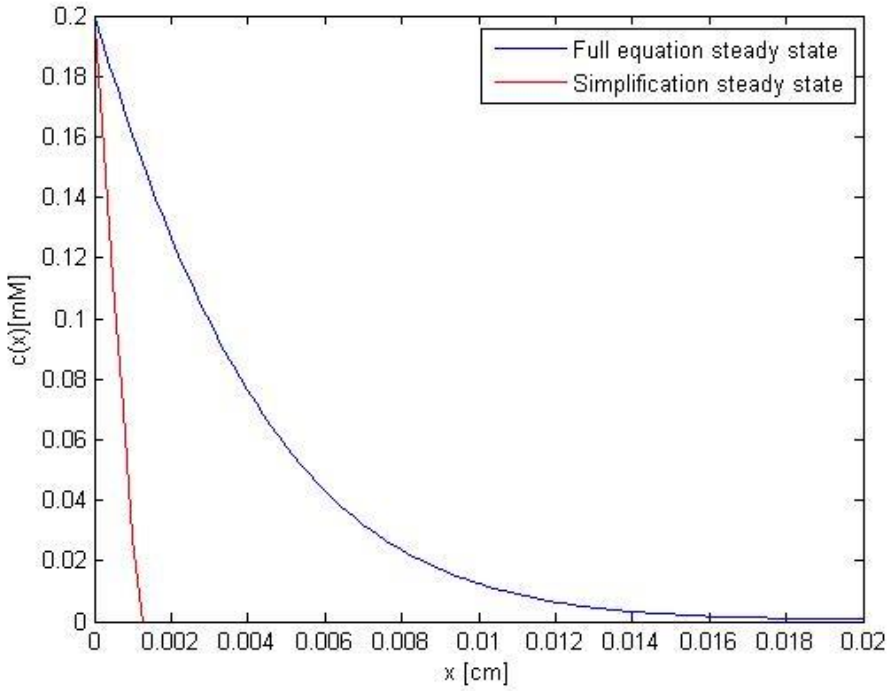

Figure 11. Steady state solution of the full equation (blue) plotted with the steady state of the simplified equation (red).

While values were not exact due to different oxygen consumption properties of different tissue types as well as assumptions we made on oxygen diffusivity, we wanted to demonstrate that the trends we found in our model matched the trends found in experimental data. Below we compare the non-linear ODE resulting from steady state oxygen consumption with oxygen consumption in rat brain slices (Figure 12A&B). The most representative curve in Figure 12B would be curve 2, which shows the extent of oxygen diffusion in post-hypoxia brain tissue. This would be the closest match to our initial conditions of 0 oxygen concentration at time t=0.

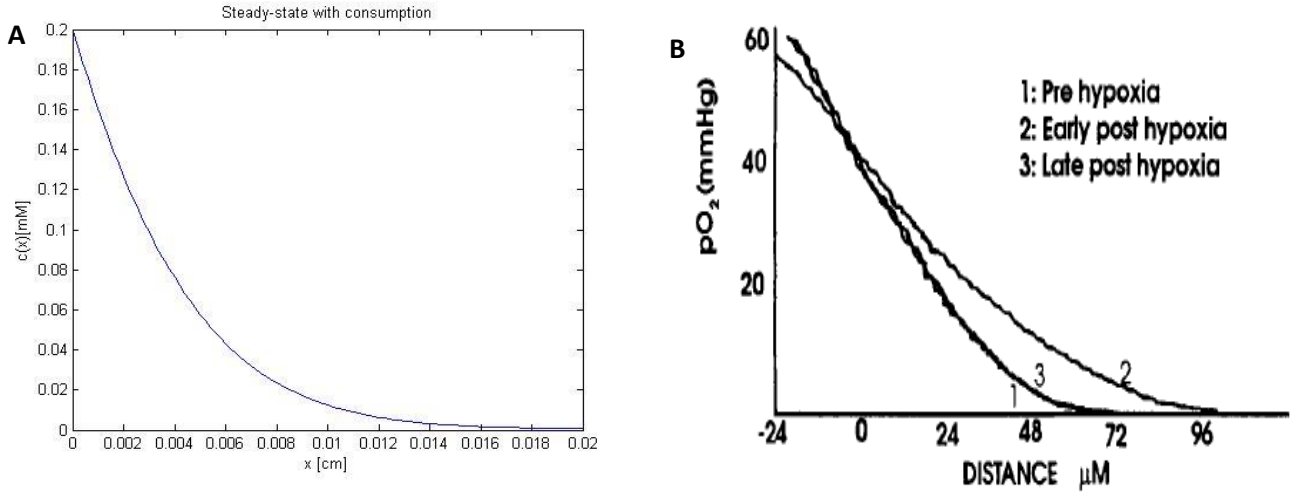

Figure 12. A: Steady state solution found using finite difference method for full equation
B: Oxygen partial pressure in slices of brain tissue against depth. (McGoron et al., 1997)

Again, due to the differences in oxygen diffusivity and consumption rates of different cell types, we observe that the concentration reaches zero around 180µm, whereas literature found that the oxygen concentration reaches zero around 80 µm. However, the general exponential decay shown in both models demonstrates the validity of our model.

Future Directions

As noted, there are a number of assumptions we made to allow us to analytically and numerically solve the model that may be invalid. The major assumption that was incorrect was that the initial concentration was zero. As shown in our graphs (Figures 5, 7, 9) there is a discontinuity at time t=0 where oxygen concentration immediately decreases from $C = C_o$ to $C = 0$. Incorporating physiological intercellular oxygen concentration would make the model more accurate.

We also did not account for the different cell layers found in skin tissue but instead assumed that the culture was homogenous. The ideal model for a skin graft would mirror the correct oxygen diffusivities, thicknesses, and consumption rates for each of these layers. In addition, the physiological intercellular oxygen concentration in each of these layers may be different. Thus, we could consider the implemetation of a series of piecewise equations that model each layer of skin.

Lastly, we assumed that oxygen consumption was independent of other biochemical activities and followed a purely Michaelis-Menten reaction kinetics. However, oxygen consumption is affected by a number of other factors such as glucose concentration[3], while V_m and K_m values change at different concentrations of oxygen as cells enter different regimes of oxygen requirements as they switch from aerobic to anaerobic respiration[12]. In reality, glucose diffuses slower than oxygen, and cell cultures are more likely to be nutrient limited rather than oxygen limited. In order to account for this relationship, a system of PDE equations can be used instead.

References

1. Bello, YM., Falabella, AF., Eaglstein, WH. "Tissue-Engineered Skin Current Status in Wound Healing." *Am J Clin Dermatol* (2001); 2 (5): 305-313.

2. Brown University. "Skin grafts and Transplants." Accessed October 25, 2013. http://biomed.brown.edu /Courses/ BI108/BI108_2007_Groups/group11/surgery.html

3. Buchwald, P. "A Local Glucose-and Oxygen Concentration-Based Insulin Secretion Model for Pancreatic Islets." *Theoretical Biology and Medical Modelling* (2011); 8(20).

4. Fournier, RL. *Basic Transport Phenomena in Biomedical Engineering, Third Edition.* Florida: Taylor and Francis Group, 2012.

5. Green H, Kehinde O, Thomas J. "Growth of cultured human epidermal cells into multiple epithelia suitable for grafting." *Proc Natl Acad Sci U S A* (1979), 76 (11): 5665-8.

6. Halim, AS., Khoo, TL., Mohd. Yussof, SJ. "Biologic and Synthetic Skin Substitutes: An Overview." *Indian J Plast Surg* (2010); 43: S23-S28.

7. Henderson, HP. "Informational Sheet Skin Grafts." Accessed October 25, 2013. http://hughhenderson.co .uk/pdfs/skin_graft.pdf.

8. Hunt TK, Pai MP. "The effect of varying ambient oxygen tensions on wound metabolism and collagen synthesis." *Surg Gynecol Obstet.* (1972); 135 (4):561–567.

9. Kwang, HL. "Tissue-engineered Human Living Skin Substitutes: Development and Clinical Application." *Yonsei Medical Journal* (2000); 41(6): 774-779.

10. McGoron, AJ., Nair, P., Schubert, RW. "Michaelis-Menten Kinetics Model of Oxygen Consumption by Rat Brain Slices following Hypoxia." *Annals of Biomedical Engineering* (1997); 25: 565-572.

11. Orgill, DP. "Excision and Skin Grafting of Thermal Burns." *The New England Journal of Medicine* (2009); 360(9): 893-901.

12. Varma, A., Boesch, BW., Palsson, BO. "Stoichiometric Interpretation of *Escherichia coli* Glucose Catabolism under Various Oxygenation Rates." *Applied and Environmental Microbiology* (1993); 59(8): 2465-2473.

Appendix A. Solution to Homogeneous PDE (No Consumption)

$$\frac{\partial c}{\partial x} = D\frac{\partial^2 c}{dx^2}$$

B.C. $c(0,t) = C_o$

B.C. $\frac{\partial c}{\partial x}(L,t) = 0$

I.C. $c(x,0) = 0$

Solution to homogeneous PDE with inhomogeneous boundary conditions can be written as the sum of the solution to the homogeneous PDE with homogeneous boundary conditions plus a particular inhomogeneous solution.

$$c(x,t) = c_H(x,t) + c_P(x)$$

Particular solution: Steady state ($t \to \infty$; $\frac{\partial C}{\partial t} = 0$)

$$D\frac{\partial^2 c_P}{\partial x^2} = 0$$

Integrating twice yields:

$$c_p(x) = c_1 x + c_2$$

Applying first boundary condition

$$c(0,t) = C_o$$

$$c_2 = c_0$$

Applying second boundary condition

$$\frac{\partial c}{\partial x}(L,t) = 0$$

$$c_1 = 0$$

Thus, the final equation for the particular solution is:

$$c_p(x) = c_0$$

Homogeneous solution

$$\frac{\partial c_H}{\partial t} = D\frac{\partial^2 c_H}{\partial x^2}$$

$$\text{B.C. } c(0,t) = 0$$

$$\text{B.C. } \frac{\partial c}{\partial x}(L,t) = 0$$

$$\text{I.C. } c(x,0) = 0$$

Separating the variables

$$c_H(x,t) = G(t).\varphi(x)$$

$$c_H(x,t) = \sum_{n=0}^{\infty} B_n \sin(\lambda x) e^{-D\lambda^2 t}$$

$$\text{where } \lambda = \frac{(2n+1)\pi}{2L}$$

Using initial conditions,

$$c(x,0) = c_0 + \sum_{n=0}^{\infty} B_n \sin(\lambda x)$$

$$B_n = \sum_{n=0}^{\infty} \frac{2}{L}\int_0^L (0 - c_0)\sin(\frac{(2n+1)\pi}{2L}x)\,dx$$

$$= -\frac{2c_0}{L}\int_0^L \sin(\frac{(2n+1)\pi}{2L}x)\,dx$$

$$= \frac{2c_0}{L}\,(\frac{2L}{(2n+1)\pi})$$

$$= \frac{4c_0}{(2n+1)\pi}$$

And the final solution is

$$c(x,t) = C_o + \sum_{n=0}^{\infty} B_n \sin(\lambda x) e^{-D\lambda^2 t}$$

where $\lambda = \frac{(2n+1)\pi}{2L}$

Appendix B. Solution to Inhomogeneous PDE (Constant Oxygen Consumption)

We developed a PDE model that accounted for oxygen diffusion and consumption. For this model we had a constant oxygen consumption term.

$$\frac{\partial c}{\partial x} = D\frac{\partial^2 c}{dx^2} - R$$

$$\text{B.C. } \mathrm{c}(0,\mathrm{t}) = \mathrm{C_o}$$

$$\text{B.C. } \frac{\partial \mathrm{c}}{\partial \mathrm{x}}(\mathrm{L},\mathrm{t}) = 0$$

$$\text{I.C. } \mathrm{c}(\mathrm{x},0) = 0$$

Where C is the oxygen concentration, x is the position through the cell layer, D is the diffusivity, and R is the constant oxygen consumption rate.

Solution to inhomogeneous PDE with inhomogeneous boundary conditions can be written as the sum of the solution to the homogeneous PDE with homogeneous boundary conditions plus a particular inhomogeneous solution.

$$c(x,t) = \ c_H(x,t) + c_P(x)$$

Particular solution: Steady state ($t \to \infty;\ \frac{\partial C}{\partial t} = 0$)

$$D\frac{\partial^2 c_P}{\partial x^2} - R = 0$$

$$\iint_{\mathbf{0}}^{x} \frac{\partial^2 c_P}{\partial x^2}\,\mathrm{dx} = \iint_{0}^{x} \frac{\mathrm{R}}{\mathrm{D}}\,\mathrm{dx}$$

Integrating twice yields:

$$c_p(\mathrm{x}) = \frac{\mathrm{R}}{2\mathrm{D}}\mathrm{x}^2 + \mathrm{cx} + \mathrm{d}$$

Applying first boundary condition

$$\mathrm{c}(0,\mathrm{t}) = \mathrm{C_o}$$

$$C_o = \frac{\mathrm{R}}{2\mathrm{D}}0^2 - \mathrm{c} * 0 + \mathrm{d}$$

$$d = C_o$$

Applying second boundary condition

$$\frac{\partial \mathrm{c}}{\partial \mathrm{x}}(\mathrm{L}, \mathrm{t}) = 0$$

$$0 = \frac{RL}{D} + c$$

$$c = -\frac{RL}{D}$$

Thus, the final equation for the particular solution is:

$$c_p(x) = \frac{R}{2D}x^2 - \frac{RL}{D}x + C_o$$

Homogeneous solution

$$\frac{\partial c_H}{\partial t} = D\frac{\partial^2 c_H}{\partial x^2}$$

$$\text{B.C. } \mathrm{c}(0, \mathrm{t}) = 0$$

$$\text{B.C. } \frac{\partial \mathrm{c}}{\partial \mathrm{x}}(\mathrm{L}, \mathrm{t}) = 0$$

$$\text{I.C. } \mathrm{c}(\mathrm{x}, 0) = 0$$

Now that we have homogeneous boundary conditions, we can apply separation of variables

See Appendix A for mathematical calculation using separation of variables

$$c_H(\mathrm{x}, \mathrm{t}) = \mathrm{G}(\mathrm{t}).\varphi(x)$$

$$c_H(x, t) = \sum_{n=0}^{\infty} B_n \sin(\lambda x) e^{-D\lambda^2 t}$$

$$\text{where } \lambda = \frac{(2n+1)\pi}{2L}$$

Full Solution

$$c(x,t) = c_H(x,t) + c_P(x)$$

Applying initial conditions

$$\text{I.C. } c(x,0) = 0$$

$$c(x,0) = 0 = c_P(x) + c_H(x,0)$$

By orthagonality of the basis functions, we solve for B_n.

$$B_n = \frac{2}{L}\int_0^L (0 - c_P(x))\sin(\frac{(2n+1)\pi}{2L}x)\,dx$$

$$= -\frac{2}{L}\int_0^L \left(\frac{R}{2D}x^2 - \frac{RL}{D}x + C_o\right)\sin(\frac{(2n+1)\pi}{2L}x)\,dx$$

$$= -\frac{R}{LD}\int_0^L x^2\sin\left(\frac{(2n+1)\pi}{2L}x\right)dx$$

$$+\frac{2R}{D}\int_0^L x\sin\left(\frac{(2n+1)\pi}{2L}x\right)dx - \frac{2C_o}{L}\int_0^L \sin(\frac{(2n+1)\pi}{2L}x\,dx$$

Using integration by parts,

$$B_n = \frac{16RL^2}{D(2n\pi+\pi)^3} - \frac{4C_O}{2n\pi+\pi}$$

And the final solution is

$$c(x,t) = \frac{R}{2D}x^2 - \frac{RL}{D}x + C_o + \sum_{n=0}^{\infty} B_n \sin(\lambda x)e^{-D\lambda^2 t}$$

where $\lambda = \frac{(2n+1)\pi}{2L}$

Appendix C: Matlab Code for Full Equation

```
C0 = 0.2; %umol/cm^3
D = 6.6*10^-6; %cm^2/s
L = 0.02;%cm
T = 100; %sec
Km = 0.075; %uM
Vm = 0.059; %uM/s


dx=(L)/100;
dt=1/500;
xmesh=0:dx:L;
tmesh=0:dt:T;
nx = length(xmesh); % number of points in x dimension
nt = length(tmesh); % number of points in t dimension
stepsize = D * dt / dx^2; % stepsize for numerical integration
sol_fd = zeros(nt, nx);
sol_fd(:,1)=sol_fd(:,1)+ C0;

for t = 2:nt
    for x = 2:nx-1
        sol_fd(t,x) = sol_fd(t-1,x) + stepsize * ...
            (sol_fd(t-1,x+1) - 2 * sol_fd(t-1, x) + sol_fd(t-1,x-1)) - ...
            Vm*dt*sol_fd(t-1,x)/(Km+sol_fd(t-1,x));
    end
    sol_fd(t,nx) = sol_fd(t, nx-1);
end

figure(1)
colormap(jet)
surf(xmesh,tmesh,sol_fd, 'EdgeColor', 'none')
title('Finite differences for full equation')
xlabel('x [cm]')
ylabel('t [s]')
zlabel('c(x,t)[mM]')

figure(2)
plot(xmesh, sol_fd(nt,:))
title('Steady-state with consumption')
xlabel('x [cm]')
ylabel('c(x)[mM]')
```